Journal of Neutron Research 24 (2022) 373–383
DOI 10.3233/JNR-220034
IOS Press


# Experimental validation of cold neutron source performance with mesitylene moderator installed at RANS

Yujiro Ikeda [a,*], Makoto Teshigawara [b], Mingfei Yan [a,*], Chihiro Iwamoto [a], Kunihiro Fujita [a], Yutaka Abe [c], Yasuo Wakabayashi [a], Atsushi Taketani [a], Takaoki Takanashi [a], M. Harada [b], Takao Hashiguchi [a], Yutaka Yamagata [a], Yoshio Matsuzaki [a], Baolong Ma [d], Masato Takamura [a], Maki Mizuta [a], Makoto Goto [a], Shota Ikeda [a], Tomohiro Kobayashi [a] and Yoshie Otake [a]

[a] *Center for Advanced Photonics, RIKEN, Wako, Saitama 351-0198, Japan*
*E-mails: yujiro.ikeda@riken.jp, mingfei.yan@riken.jp*
[b] *J-PARC Center Japan Atomic Energy Agency, Tokai-mura, Naka-gun, Ibaraki 319-1195, Japan*
*E-mail: teshigawara.makoto@jaea.go.jp*
[c] *Kyoto University, Kyotodaigaku-Katsura Nishikyou-ku Kyoto 615-8530, Japan*
[d] *School of Energy and Power Engineering, Xi'an Jiaotong University, Xi'an, China*

**Abstract.** The RANS (RIKEN Accelerator driven Neutron Source), one of compact accelerator neutron sources (CANS), tries to expand its performance by installing a cold neutron which may provide new opportunities in many applications. RANS is a low power CANS with a proton beam of 7 MeV and 100 μA at maximum. A moderator system was constructed based on results of optimization design study with mesitylene. Recently, we have done performance tests aiming at showing characteristics as cold neutron source. Cryogenic mesitylene moderator was installed on a plug with a new target moderator reflector configuration of RANS. Experiment using a gas electron multiplier (GEM) detector was carried out to measure neutron spectra of the cold moderator. This paper describes performance of the cold moderator in terms of 1) Cold neutron gain of optimization design with respect to a polyethylene moderator, 2) Temperature dependency of cold neutron spectrum flux regarding scattering kernel (SK), and 3) comparison between experiment and calculation. A note is given for comparison between calculations with different SKs available. Also, two-dimensional imaging of cold and thermal neutron spectrum flux on the viewed surface is shown with a pinhole slit configuration.

Keywords: Cold neutron, mesitylene moderator, RANS, scattering kernel, GEM detector

## 1. Introduction

A cryogenic system for cold neutron moderator has been newly installed in the target station of RANS (Riken Accelerator driven Neutron Source) [1–3], one of compact accelerator neutron sources, to meet requests from many user applications. Neutrons are generated via the $^{9}$Be(n,p)$^{9}$B reaction at a beryllium target with 7 MeV proton injection. Mesitylene was chosen as the moderator material for cold neutrons. Number of studies on characteristics of mesitylene moderator have been reported [4–7]. Extensive studies on the proper cold neutron increase by testing configurations mesitylene moderator cope with water pre-moderators have been reported at the IBR reactor at Dubna [8]. They found considerably large gain of cold neutrons up to a factor of 10 is to be provided. Recently, Tasaki, et al, reported neutron spectrum temperature dependency for a mesitylene moderator system with a wing geometry using a p-Be neutron source [9]. The results clearly indicated that as temperature becomes below 30 K,

*Corresponding authors. E-mails: yujiro.ikeda@riken.jp, mingfei.yan@riken.jp.

neutrons with long wavelength could be provided efficiently. The RANS cold moderator has a particular challenge in a slab geometry providing both fast and slow neutron in the forward direction.

Taking the RANS target, moderator reflector (TMR) configuration into consideration, the system was designed based on optimization results [10] without changing the RANS principal frame structure. A plug system was devised to enable insertion of the cryogenic moderator from the front of the target assembly, which makes the system maintenance efficient and easy without hard labor of shielding removal. The system was constructed to meet all critical conditions for the cryogenic moderator base after a reformation of the RANS target station from the old structure by replacing mainly borated polyethylene (BPE) at the central zone with polyethylene (PE) and adding a volume of graphite reflector around moderator region, aiming at both increase of thermal neutron along neutron beam line, and reduction of fast neutron in the forward direction. Also, some of extension of collimator at the exit of beam extraction, we have layered BPE structure to make clear cut of the neutron beam profile. Given the overall system structure and the hardware of mesitylene moderator devise, this paper describes mainly neutronics performance of the cold moderator in terms of 1) cold neutron gain of optimization design from PE moderator, 2) temperature dependency of cold neutron spectrum flux regarding neutron scattering kernel (SK) data and 3) comparison neutron spectrum in thermal to cold region between experiment and calculation in absolute flux intensity fashion. Discussion is made on the adequacy of the SK data used in simulation. Also, characteristics of cold neutron extraction is shown based on the results for measurement of two-dimensional neutron flux distribution on the viewed surface of mesitylene moderator.

## 2. RANS cold moderator system

A drawing of vertical cross-sectional view at the center of current RANS is shown in Fig. 1 for understanding configuration of the cold cryogenic moderator system on a plug.

Major dimensions of the newly constructed RANS assembly with plug structure as given in Fig. 1 are closely related to the configuration of the cryogenic mesitylene moderator system. As we keep the same opening of 150 × 150 mm$^2$ for neutron beam extraction port of the old RANS [1–3], a size of the moderator viewed surface was decided to be 100 × 100 mm$^2$ to be able to attach pre-moderator. The PE pre-moderator layers with thicknesses of 30 mm and 15 mm at the rear and side and bottom of the moderator vessel, respectively, are configured. An

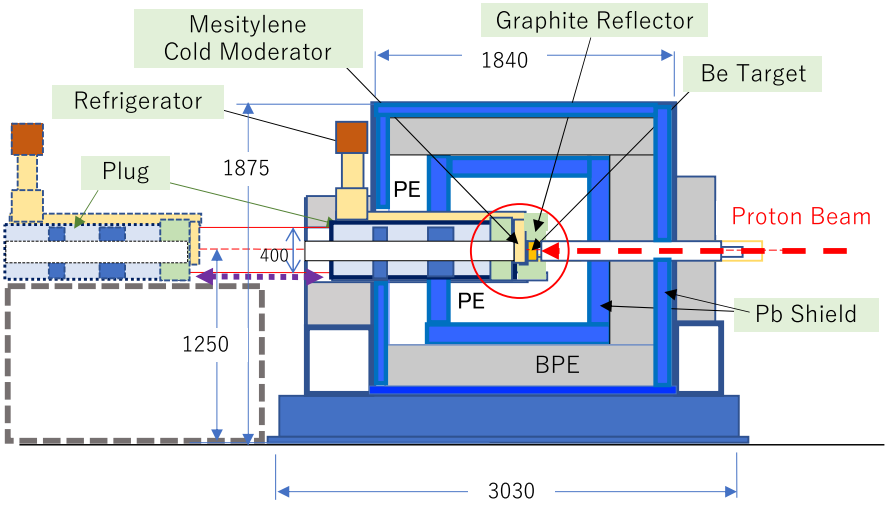


Fig. 1. Schematic drawing of a vertical cross section of the RANS target assembly. Unit of numerical values is in mm. A horizontal cut view of region within red colored circle at around the center of assembly is given in Fig. 2.

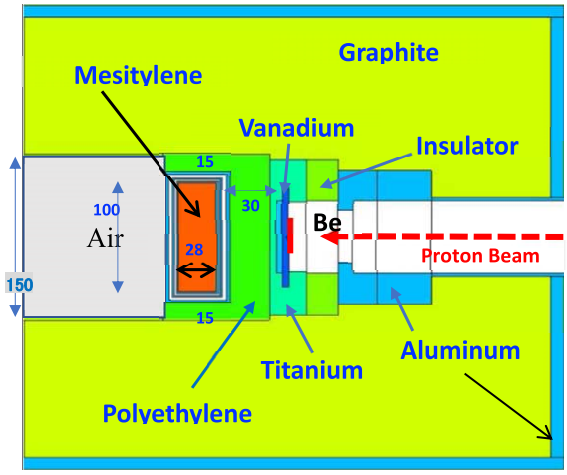


Fig. 2. Horizontal cut view of the target/moderator/reflector configuration. Mesitylene cryogenic cold moderator surrounded polyethylene pre-moderator is attached to the Be target structure. Unit of numerical value is given in mm.

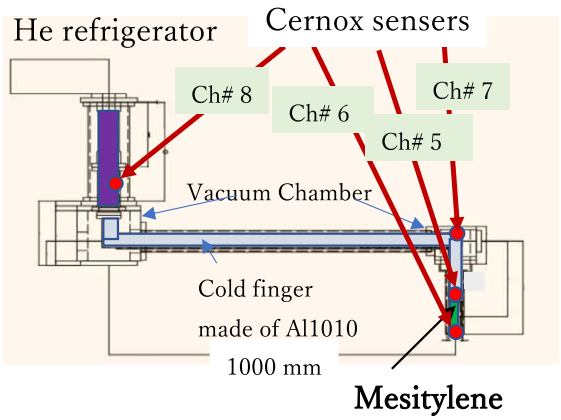


Fig. 3. Vertical cut view of the cryogenic moderator system components. Red dots are position of the temperature.

expanded view for materials structure of the Be neutron production target/mesitylene cold moderator/graphite reflector with major dimensions are shown in Fig. 2. The moderator vessel is made of Al-1050.

Figure 3 shows a vertical cut of the cryogenic moderator system comprised with a refrigerator, cold bar for heat conduction, moderator vessels with moderator indicating attached temperature sensors. The core mesitylene region is thermally insulated by intermediate layer of 1 mm thick Al plate and super-insulator made of Al deposited polyimide films with embossed treatment (Ube-Kousan LTD), which are inserted in spaces between both the core vessel and the intermediate layer, and the intermediate layer and vacuum vessel. At least, five layers of SI films were kept in between the chamber walls covering the viewed surface of the moderator. Mesitylene (1, 3, 5-trimethylbenzene) $C_9H_{12}$, which has a melting point at $-45$°C and density of 0.86 g/cm$^3$ at room temperature was confined in an Al container that has a volume of $93.5 \times 93.5 \times 27.5$ (mm$^3$). From the net weight of measured 195.7 g, about 98% of volume of the vessel was estimated to be filled with the mesitylene. Cooling down of the system was carried out by using a refrigerator (Suzuki-Shokan model: RF70D) connected through heat transfer lines with a water cooled He compressor (SSC-3700). The cold head was connected thermally to the moderator vessel through Cu and Al links in a vacuum chamber as shown in Fig. 3. To monitor temperature of the moderator,

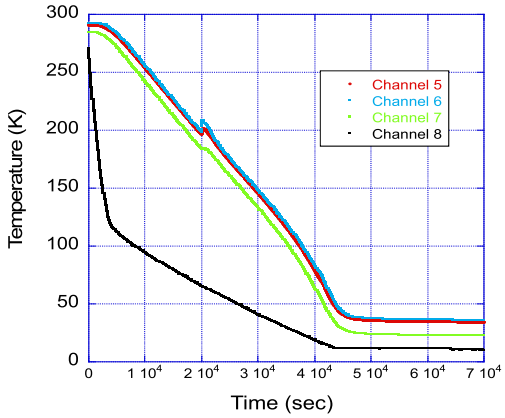


Fig. 4. Curves of temperature change of four sensors. Temperature of mesitylene was estimated to be 32.5 K corresponding to sensors of channels 5 and 6.

several temperature sensors for low temperature, called as Cernox (Lake Shore Cryotronics, Inc.), were attached on top and bottom surfaces of the Al moderator vessel, on the Cu cold bar just upper position of the moderator, and on the Cu cold head of the refrigerator as shown in Fig. 3. During cooling of the system, temperatures were recorded by using the 182-module of Lake Shore Cryotronics, Inc. Figure 4 is a plot showing temperature changes during cool down process.

## 3. Experimental

In viewing the importance of neutronic performance, we have measured neutron spectra on several different temperatures of 290 K, 230 K, 160 K, 83 K, and 32.5 K at a position of about 2.4 m from the Be target by using the time of flight (TOF) technique with a gas electron multiplier (GEM) detector for neutron. It has 128 $\times$ 128 pixels with 1 mm spatial resolution. Effective detection area is 100 $\times$ 100 mm$^2$. Temperature dependency of neutron spectra at cold neutron energy region are clearly observed. Along with the neutron spectrum, ratios of reaction rates of the $^{197}$Au(n, $\gamma$)$^{198}$Au with and without Cd cover were measured at some temperatures.

Also, two-dimensional image of the cold neutron distribution on the moderator viewed surface was taken using a pinhole slit made of $B_4C$ containing rubber by using the GEM detector. Neutron spectrum at 2.4 m distance from the Be target was measured by TOF with the GEM detector. Neutrons were extracted through a guide channel, so that all neutrons from viewed surface of the moderator and interacted with materials along the channel contributed neutron spectrum at the detector.

### *3.1. Detector efficiency calibration*

Neutron detection efficiency was obtained by using a calibrated $^3$He one-dimensional counter. TOF spectra were taken by these two detectors placing at the same position. They are shown in Fig. 5 along with that calculated by MCNP [11]. In this study, we assumed the efficiency of the $^3$He counter calibrated at 25 meV is the base for that of the GEM.

There are rather reasonable agreements with that obtained by the MCNP calculation throughout time range although slightly difference in an energy range of less than 10 meV. Finally, the detector efficiency of the GEM detector is almost 4% of the neutron energy range from 100 meV to 2 meV. It is found that the efficiency is slightly low at energy below 1 meV relative to that of the $^3$He detector.

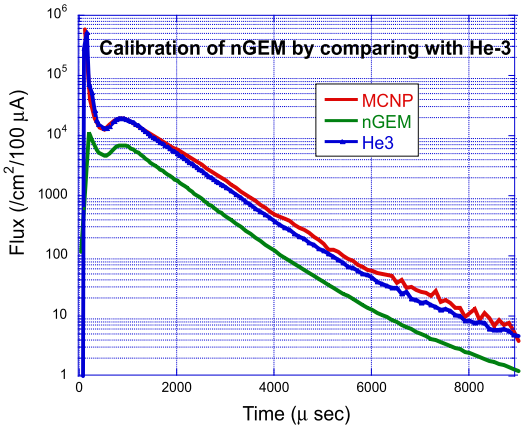


Fig. 5. Time spectra for detection efficiency calibration of the reference $^{3}$He detector, GEM, $^{3}$He and MCNP calculation.

### *3.2. Neutron spectrum measurement*

Neutron spectra emitted the moderator of different temperatures from room temperature (RT) to 32.5 K are shown in Fig. 6, which were reduced from the measured time of flight (TOF) spectra. Also, a spectrum from a PE moderator, which dominantly provides neutron of thermal energy at around several tens meV, is shown in Fig. 6 for comparison. The comparison is of help to understand how the mesitylene cold moderator decreases neutron energy and increases intensity in a neutron energy range below 10 meV. Experimental errors include those of statistics of the counts, the detector efficiency and neutron productions, as less than ±1%, ±4% and ±6%, respectively. The change in the neutron energy with different temperature is consistent with previous reports [8,9]. It is notable that a gain in the neutron intensity at around 1 meV is a factor of 4 to 5 to that of PE moderator case, although it is rather small compared with that about 6 obtained by design optimization study [10].

## 4. Calculation and discussion

### *4.1. Code and data*

Neutron flux spectra corresponding to those measurements are calculated with MCNP6 [11], where ENDF/B-VII nuclear data library [12] is used. It is noted that in an energy rage below 1 eV, the scattering kernel data must be used as far as they are available to predict scattering events in the energy range, where possible energy transfer with neutrons is expected. The scattering is characterized by the materials structure, crystallization, chemical formation. Thus, neutron scattering kernels corresponding to temperatures as measured were created by taking all information by Abe *et al*. [13]. Figure 7 shows neutron spectra calculated by using the scattering kernels.

### *4.2. Comparison with experiments*

From Figs 6 and 7, good agreements are identified in terms of temperature dependency, their orders peak energies. The spectrum for a moderator with 40 mm thick polyethylene is also given in these figures for comparison. It is clearly demonstrated that the cold mesitylene produces appreciable amounts of cold neutron below 10 meV and could serve as cold neutron source even its intensity is low compared with solid methene. It is also suggested that the neutron flux spectrum is consistent with those in the optimization study [10]. It should be noted that measurements are systematically lower by around 15% to 20% than calculations with MCNP calculation using ENDF/B-VII nuclear data. A possible explanation for this difference is discussed in Section 5 later from the neutron production cross section point of view.

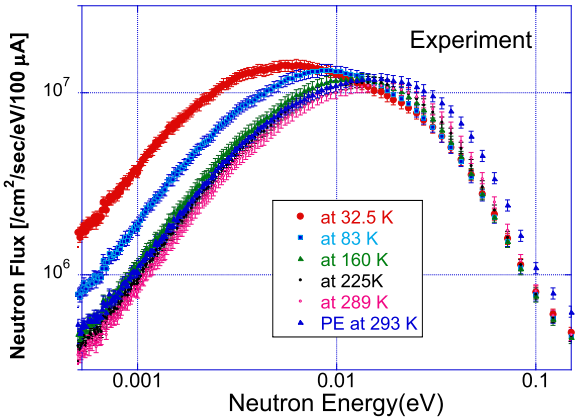


Fig. 6. Temperature dependent neutron spectra below 0.2 eV measured by GEM.

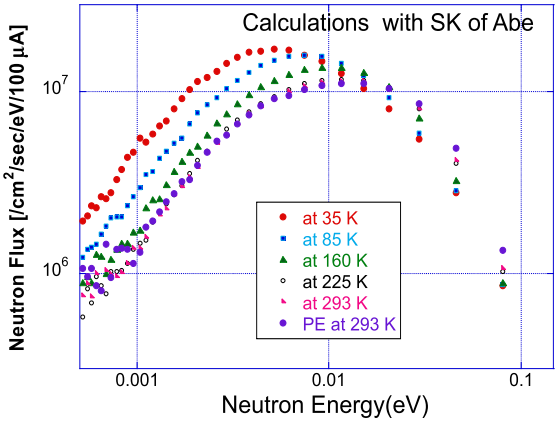


Fig. 7. Temperature dependent neutron spectra below 0.2 eV calculated by MCNP with SK of Abe.

### *4.3. Cd ratio of reaction rate of the $^{197}$Au(n, $\gamma$)$^{198}$Au reaction*

As it was suggested that temperature decrease of mesitylene increases slowing down of neutron to be less energy neutron, the ratio of the $^{197}$Au(n, $\gamma$)$^{198}$Au reaction with a Cd cover to that without it. Measurement of gold foil activation with and without the Cd at 100 mm distance from the moderator surface was carried out in three cases with difference temperatures of mesitylene at 293, 110 and 32.5 K. In addition to those cases, measurements for the 40 mm thick PE moderator at 293 K as a reference to evaluate cold neutron performance. Reaction rates were calculated with MCNP by using Abe's SK. For both measurements and calculations, ratios shown in Fig. 8 clearly indicate a dependency of the Cd ratio, which closely related with cold neutron increase, on mesitylene temperature. This is a demonstration of the cold neutron formation in the cryogenic mesitylene moderator. As the temperature of experimental measurement was identified to be 32.5 K, the absorption could be a bit smaller than that at 20 K. The slightly large deviation between calculation and measurement suggests it.

### *4.4. Comparison of neutron scattering kernel*

There are two scattering kernel data available for the analysis. We call one of them as Granada, which was provided by Granada et al. [14,15], and the other as Abe [13]. Unfortunately, as the data of Granada is just for 20 K

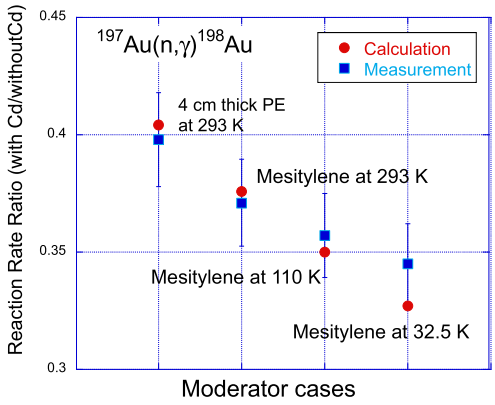


Fig. 8. Ratios of reaction rate of the $^{197}$Au(n, $\gamma$)$^{198m}$Au reaction. with Cd cover to that without, at different mesitylene temperatures. A value for 4 cm thick polyethylene moderator is plotted for a reference.

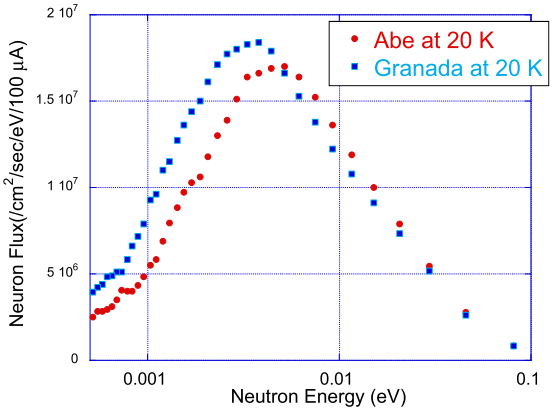


Fig. 9. Comparison of neutron spectra calculated by using SKs of Abe and Granada in an energy region below 10 meV.

temperature, a comparison was made for the neutron spectra at the same conditions for the simulation by using Abe and Granada. From spectra compared in Fig. 9, a good agreement at above 100 meV is found. However, difference become significant as energy decrease to the cold neutron region down to 0.2 meV. Also, it is pointed out that Granada give stronger slowing down by mesitylene than Abe. Granada gives about 20% higher neutron flux below 10 meV than Abe does. This amount difference is appreciably large for evaluation of the source characteristics point of view.

Although this experimental study currently looks supportive to Abe's SK, there are still several critical concerns to be identified in terms of the mesitylene phase state. Firstly, we assumed that according to that phase diagram of mesitylene [16], mesitylene at temperatures of 32.5 K and 85 K below 90 K stayed in stable phase of Phase-III. Mesitylene at 160 K was thought to be in Phase-II as phase transition is assumed to occur when temperature change passed at 90 K when it was warmed. Furthermore, as the phase transfer from Phase-II to Phase-I at 190 K, mesitylene at 225 K was in Phase-I.

Based on above identification, a brief discussion is given for kernels of Abe and Granada as follows: The kernel was made by using the molecular dynamics model. Behavior of density of state for bound rotation of methyl group is rather intermediate between that of Phase-II including Phase-I, and Phase-III. On the other hand, the kernel of Granada was made for Phase-II, which is available in the JEFF-3.3 nuclear data library [17]. This may indicate that Granada kernel tend to give slower neutron energy spectrum than that by using Abe kernel as shown in Fig. 9.

Measurement at 32.5 K, which were assumed to be that of Phase-III, was in a good agreement with calculation with Abe kernel at 35 K although corresponding temperatures were slightly different. It is due to calculation with Abe kernel, as noted before, showing an intermediate character between Phase-II and III as shown in Fig. 6 and Fig. 7. Concerning the SK of Granada which may correspond to the Phase-II model of mesitylene at 20 K. Even though, the temperature is lower than 32.5 K in the measurement, it is anticipated that the calculated neutron spectrum exhibited a large shift to lower energy side. Still there is, however, a possible discussion on determination of absolute value of density of state.

## 5. Absolute neutron flux prediction via C/E with JENDL-5 nuclear data library

Lastly, it is notable that the nuclear data of JENDL-5 [18] suggested a significant improvement in the prediction accuracy in any neutron flux simulation at the p-Be for RANS neutron production source. So far, neutron spectrum is calculated by using a source neutron production routine, called as Waka-func, at RANS. It was suggested already in paper [19] which summarized that data used Waka-func overestimated by about 15% the experiment. According to this conclusion, JENDL-5 seems reasonable reduction of Waka-func as far as p-Be reaction is concerned, in its evaluation process. Figure 10 shows the neutron spectrum at a 10 cm distance from the Be target. Integral Intensity calculated by using PHITS code [20] with the nuclear data of JENDL-5 is lower than that with Waka func. This result indicates that overestimation in all neutron flux spectrum calculation is attributable to RANS neutron source based on the Waka-func which could be slightly overestimated experiments, and it is consistent with the JENDL-5 nuclear data.

## 6. Neutron flux distribution

To investigate more in detail neutron flux distribution on the viewed surface of the moderator, we have measured the profile by using a pinhole geometry beam configuration as shown in Fig. 11, in which twice as large image is projected on the GEM detector. The GEM detector obtained both 2-dimensional image of the energy dependent flux distribution. Figure 12 shows the pin-hole image of the moderator in two different neutron energy ranges (from 0.2 to 10 meV on the left, and above 10 meV on the right). There is clear difference in region of respective neutron emission, Emphasis is placed on the central region corresponding to the mesitylene, which is in a good agreement

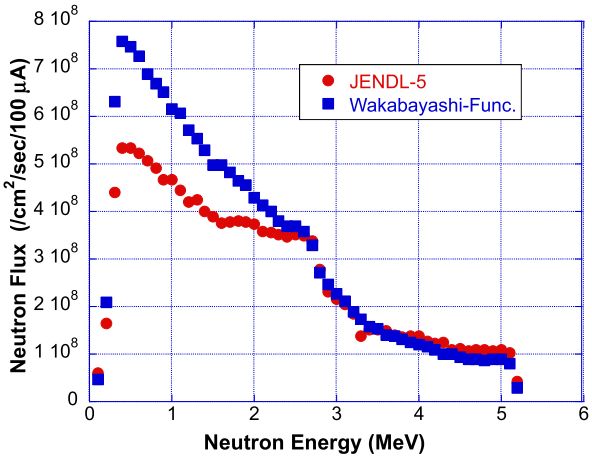


Fig. 10. Neutron source spectra at a position of 100 mm in forward direction from a Be target center calculated by PHITS with Waka-func and JENDL-5 for neutron production via the $^{7}$Be(p,n) reaction with 7 MeV proton injection.

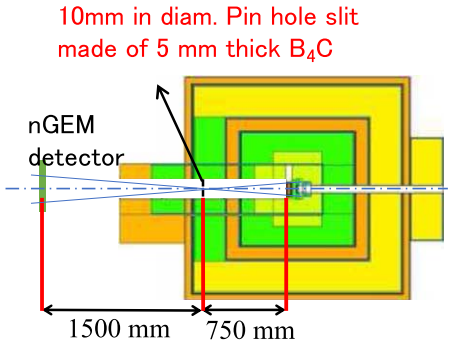


Fig. 11. Configuration of the pinhole image measurement. Distance ratio of the detector and the pinhole was 3:2, giving a factor of 2 enlargement.

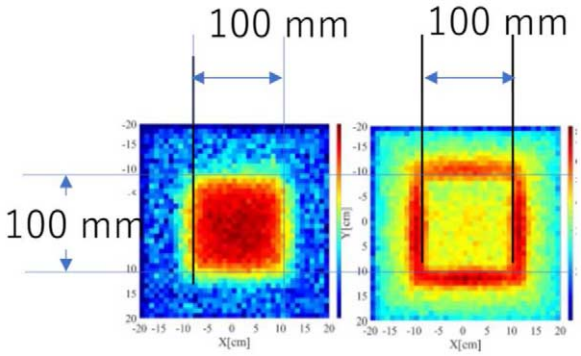


Fig. 12. Two-dimensional image of neutron flux intensities corresponding to energy regions below; "1 meV < En < 10 meV" and "10 meV < En < 200 meV".

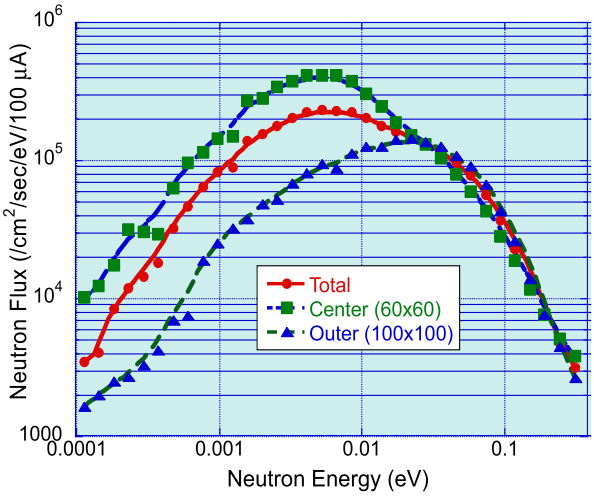


Fig. 13. Neutron spectra extracted from central region and outer region of the moderator viewed surface.

with the simulation result. The rectangular frame like zone appeared in the thermal neutron image from PE pre-moderator, described in the previous section for the structure of the moderator. As shown in Fig. 13, neutron spectra from this viewed surface are corresponding to cold and thermal neutrons. The data implies that the extraction of cold neutron or a bi-spectrum neutron could be contourable by applying appropriate slits or collimators.

## 7. Concluding remarks

There are several important outcomes from performance test of the newly installed mesitylene cold neutron source at RANS, as follows:

0) The plug system is effective in installation of the cryogenic moderator,
1) Flux spectrum comparison between experiment and calculation indicated that the SK by Abe was adequate in the first Phase of mesitylene at 20 K.
2) Cold neutron flux gain of optimization design was confirmed.
3) Temperature dependency of cold neutron spectrum flux was demonstrated by experiment and calculation using SK.
4) Two-dimensional imaging of cold and thermal neutron spectrum fluxes on the viewed surface might provide a guide to devise an effective neutron beam extraction.
5) Lastly, the nuclear data of JENDL-5 suggested a significant improvement in the prediction accuracy in any neutron flux simulation at the p-Be based RANS.

In conclusion, based on the mesitylene cryogenic moderator system operation, cold neutron flux in the energy range less than 5 meV down to 0.2 meV is now available in applications, such as small angel scattering, and transmission, and so on at RANS.

## Acknowledgement

Authors express their thanks for all member of RANS facility to support experiments. Also. Neutronics section group of J-PARC center participated encouraging discussion on the cold neutron formation.

## References

[1] Y. Otake, RIKEN compact neutron systems with fast and slow neutrons, *Plasma Fusion Res.* **13** (2018), 2401017. doi:10.1585/pfr.13.2401017.
[2] Y. Otake, RIKEN accelerator-driven compact neutron systems, *EPJ Web Conf.* **231** (2020), 01009. doi:10.1051/epjconf/202023101009.
[3] Y. Ikeda, A. Taketani, M. Takamura, H. Sunaga, M. Kumagai, Y. Oba, Y. Otake and H. Suzuki, Prospect for application of compact accelerator-based neutron source to neutron engineering diffraction, *Nucl. Instrum. Methods Phys. Res., Sect. A* **833** (2016), 61–67. doi:10.1016/j.nima.2016.06.127.
[4] Y. Kiyanagi, Experimental studies on neutronic performance of various cold-neutron moderators for the pulsed neutron sources, *Nuclear Instruments and Methods in Physics Research Section A: Accelerators, Spectrometers, Detectors and Associated Equipment* **562** (2006), 561–564. doi:10.1016/j.nima.2006.02.009.
[5] Y. Kiyanagi, K. Tagaya, T. Chiba, H. Iwashita, F. Hiraga and T. Kamiyama, Neutronic studies on a grooved moderator for a small accelerator-based neutron source by Monte Carlo simulation, in: *ICANS XIX, 19th Meeting on Collaboration of Advanced Neutron Sources*, Grindelwald, Switzerland, March 8–12, 2010.
[6] C.M. Lavelle', D.V. Baxter, A. Bogdanov, V.P. Derenchuk, H. Kaiser, M.B. Leuschner, M.A. Lone, W. Lozowski, H. Nann, B.V. Przewoski, N. Remmes, T. Rinckel, Y. Shin, W.M. Snow and P.E. Sokol, Neutronic design and measured performance of the Low Energy Neutron Source (LENS) target moderator reflector assembly, *Nuclear Instruments and Methods in PhysicsResearch A* **587** (2008), 324–341. doi:10.1016/j.nima.2007.12.044.
[7] K. Unlu et al., The University of Texas Cold Neutron Source, *Nuclear Instruments and Methods, A* **353** (1994), 397. doi:10.1016/0168-9002(94)91684-5.

[8] S. Kulikov, V. Ananiev, A. Belyakov, M. Bulavin, K. Mukhin, A. Rogov, E. Shabalin and A. Verkhoglyadov, Proc. Int. Conf. Neutron Optics (NOP2017), *JSP Conf. Proc.* **22** (2018), 011001.
[9] S. Tasaki, Y. Idobata, Y. Adachi, F. Funama and Y. Abe, Study on moderation properties of cold mesitylene using KUANS, *EPJ Web Conferences* **232** (2020), 04005, UCANS-8.
[10] B.L. Ma, M. Teshigawara, Y. Wakabayashi, M.F. Yan, T. Hashiguchi, Y. Yamagata, S. Wang, Y. Ikeda and Y. Otake, Optimization of a slab geometry type cold neutron moderator for RIKEN accelerator-driven compact neutron source, *Nuclear Instruments and Method, A* **995**(11) (2021), 165079. doi:10.1016/j.nima.2021.165079.
[11] T. Goorley, MCNP6.1.1-beta release notes, LA-UR-14-24680, 2014.
[12] M.B. Chadwick, ENDF/B-VII.0: Next generation evaluated nuclear data library for nuclear science and technology, *Nuclear Data Sheets* **107**(12) (2006), 2931–3060. doi:10.1016/j.nds.2006.11.001.
[13] Y. Abe et al., Development of a general-purpose code for analyzing thermal neutron scattering cross-sections of hydrogenous molecules by molecular dynamics, to be submitted.
[14] J.R. Granada and F. Cantargi, Development of cold neutron scattering kernels for advanced moderators, *AIP Conference Proceedings* **1202** (2010), 8. doi:10.1063/1.3295617.
[15] J.R. Granada, R.E. Mayer, J. Dawidowski, J.R. Santisteban, F. Cantargi, J.J. Blostein, L.A. Rodr´ ıguez Palomino and A. Tartaglione, The sciences and applications of the electron LINAC-driven neutron source in Argentina, *Eur. Phys. J. Plus* **131** (2016), 216. doi:10.1140/epjp/i2016-16216-2.
[16] I. Natkaniec and K. Holderna-Natkaniec, Structural phase transitions and dynamics of slid mesitylene investigated by diffraction and inelastic neutron scattering method, in: *Proceedings of ACoM 6 (6th Meeting of the Collaboration on Advanced Cold Moderators)*, Jeulich, Germany, 11–13 September, 2002.
[17] A.J.M. Plompen et al., The joint evaluated fission and fusion nuclear data library, JEFF-3.3, *The European Physical Journal A* **56** (2020), Article ID 181.
[18] S. Kunieda, K. Yamamoto, C. Konno, Y. Iwamoto, O. Iwamoto, Y. Wakabayashi and Y. Ikeda, Estimation of double-differential cross-sections of $^{9}$Be(p, xn) reaction for new nuclear data library, in: *JENDL-5, Presented UCANS9*, March, 2022.
[19] Y. Wakabayashi, A. Taketani, T. Hashiguchi, Y. Ikeda, T. Kobayashi, S. Wang, M.F. Yan, M. Harada, Y. Ikeda and Y. Otake, A function to provide neutron spectrum produced from the $^{9}$Be + p reaction with protons of energy below 12 MeV, *Journal of Nuclear Science and Technology* **55**(8) (2018), 859–867. doi:10.1080/00223131.2018.1445566.
[20] T. Sato, L. Sihver, H. Iwase, H. Nakashima and K. Niita, Simulations of an accelerator-based shielding experiment using the particle and heavy-ion transport code system PHITS, *Adv. Sp. Res.* **35**(2) (2005), 208–213. doi:10.1016/j.asr.2005.01.041.